# Effects of rotation and magnetic field on the nonlinear peristaltic flow of a second-order fluid in an asymmetric channel through a porous medium

A. M. Abd-Alla[a)b)†], S. M. Abo-Dahab[a)c)], and H. D. El-Shahrany[a)]

[a)] *Department of Mathematics, Faculty of Science, Taif University, Saudi Arabia*
[b)] *Department of Mathematics, Faculty of Science, Sohag, Egypt*
[c)] *Department of Mathematics, Faculty of Science, South Valley University, Qena* 83523, *Egypt*

(Received 22 October 2012; revised manuscript received 15 January 2013)

In this paper, the effects of both rotation and magnetic field of the peristaltic transport of a second-order fluid through a porous medium in a channel are studied analytically and computed numerically. The material is represented by the constitutive equations for a second-order fluid. Closed-form solutions under the consideration of long wavelength and low Reynolds number is presented. The analytical expressions for the pressure gradient, pressure rise, friction force, stream function, shear stress, and velocity are obtained in the physical domain. The effects of the non-dimensional wave amplitude, porosity, magnetic field, rotation, and the dimensionless time-mean flow in the wave frame are analyzed theoretically and computed numerically. Numerical results are given and illustrated graphically in each case considered. Comparison was made with the results obtained in the presence and absence of rotation, magnetic field, and porosity. The results indicate that the effects of the non-dimensional wave amplitude, porosity, magnetic field, rotation, and the dimensionless time-mean flow are very pronounced in the phenomena.

**Keywords:** peristaltic flow, second-order fluid, magnetic field, porous medium

**PACS:** 47.15.G–, 47.15.Rq, 47.27.nd, 47.45.Gx **DOI:** 10.1088/1674-1056/22/7/074702

## 1. Introduction

Peristalsis is defined as a wave of relaxation/contraction imparted to the walls of a flexible conduit, thereby pumping the enclosed material. Investigations of the peristaltic flow of a fluid in a channel induced by a wave traveling on its wall have many applications in various branches of science. The physical mechanism of the flow induced by the traveling wave can be well understood and is known as the peristaltic transport mechanism. This mechanism is a natural cause of motion of fluids in the body of living creatures, and it frequently occurs in organs such as ureters, intestines, and arterioles. The mechanism of peristaltic transport has been exploited for industrial applications like sanitary fluid transport, blood pumps in heart lung machines, and transport of corrosive fluids where the contact of the fluid with the machinery parts is prohibited. In recent years, considerable efforts have been usefully devoted to the study of peristaltic flow of non-Newtonian fluids because a practical and fundamental constitutive relation that can be used for all fluids and flow is not available. Hayat *et al.*[1] investigated the effects of different wave forms on the peristaltic flow of micropolar fluids through a channel, and reported that the maximum pressure against which peristalsis works increases with the coupling number but decreases with the micropolar parameter. Siddiqui and Schehawey[2] analyzed the mechanics of peristaltic pumping of non-Newtonian fluid through an axisymmetric conduit. Abd-Alla *et al.*[3] presented the time mean axial velocity profiles in the case of free peristaltic pumping and analyzed the influence of wall properties, magnetic field, rotation and initial stress for various values of micropolar fluid parameters of peristaltic flow. Mahmoud *et al.*[4] discussed the effect of the rotation on the wave motion through a cylindrical bore in a micropolar porous medium. Tripathi *et al.*[5] studied the peristaltic transport of a generalized Burgers' fluid, and discussed the applications in the movement of chyme in small intestines. Wang *et al.*[6] investigated the magnetohydrodynamic flow of an incompressible electrically conducting micropolar fluid in a circular tube with a sinusoidal wave of small amplitude traveling down its wall. Akbar *et al.*[7] discussed the influence of heat and mass transfer on the peristaltic flow of a hyperbolic tangent fluid in an annulus. Akbar *et al.*[8] investigated the effects of slip and heat transfer on the peristaltic flow of a third-order fluid in an inclined asymmetric channel. Gad[9] studied the effect of Hall current on the peristaltic flow of particle fluid suspension. Nadeem and Akbar[10] studied the effects of the induced magnetic field and heat and mass transfer on the peristaltic flow of Johnson–Segalman fluid in a vertical asymmetric channel. Hayat *et al.*[11] discussed the effect of an induced magnetic field on peristaltic flow of an incompressible Carreau fluid in an asymmetric channel. Pandey *et al.*[12] studied the peristaltic transport of multilayered power-law fluids with distinct viscosities. Pandey *et al.*[13] presented a peristaltic flow of

†Corresponding author. E-mail: mohmrr@yahoo.com

© 2013 Chinese Physical Society and IOP Publishing Ltd 

a Williamson model in an asymmetric channel. Pandey and Chaube[14] studied the peristaltic transport of a visco-elastic fluid in a tube of non-uniform cross section. Haroun[15] considered the effects of Deborah number and phase difference on the peristaltic transport of third-order fluid in an asymmetric channel. Kothandapani and Srinivas[16] investigated the peristaltic transport of an incompressible viscous fluid in an inclined asymmetric channel through a porous medium under assumptions of long wavelength and low Reynolds number. Hayat *et al.*[17] also examined the peristaltic transport of a third-order fluid under the effects of transverse magnetic field. Ali *et al.*[18] also examined the peristaltic flow of third grade fluid in a curved channel. Hayat and Ali[19] investigated the effect of magnetic field on peristaltic transport of a Jeffrey fluid through a tube. They concluded that the pressure rise per wavelength and friction force per wavelength increase with the Hatman number. Kothandapani and Srinivas[20] discussed the magnetohydrodynamic (MHD) peristaltic flow of Jeffrey fluid in an asymmetric channel. Haroun[21] studied the non-linear peristaltic flow of a fourth grade fluid in an inclined asymmetric channel. Hayat *et al.*[22] investigated the peristaltic motion of an MHD non-Newtonian fluid in an inclined asymmetric channel in the presence of a constant inclined magnetic field making an angle with the vertical axis with assumptions of long wavelength and low Reynolds number. The influence of inclined magnetic field on the peristaltic flow of a Williamson fluid in an inclined symmetric or asymmetric channel has been investigated initially in the wave frame of reference by Nadeem and Akram.[23] Srinivas and Gayathri[24] discussed the problem of the peristaltic flow of a Newtonian fluid with heat transfer in a vertical asymmetric channel through porous medium under assumptions of long wavelength and low Reynolds number. Srinivas and Pushparaj[25] have investigated the peristaltic pumping of the MHD gravity flow of a viscous incompressible fluid in a two-dimensional asymmetric inclined channel having electrically insulated walls. An infinite train of peristaltic waves under conditions for which the relevant Reynolds number is small enough for inertial effects to be negligible and the wavelength to diameter ratio is large enough for the pressure to be considered uniform over the cross-section is investigated by Shapiro *et al.*[26] Shukla *et al.*[27] studied the effects of peripheral layer viscosity on physiological characteristics of a bio-fluid due to peristaltic transport through the artery with mild stenosis. It is shown that, for a given pressure drop, the flow flux increases and the frictional force decreases as the viscosity of the peripheral-layer fluid decreases.

The aim of the present paper is to discuss the peristaltic flow of a second-order fluid through a porous medium in a two-dimensional channel. The fluid is electrically conducted in the presence of a magnetic field with rotation. The governing equation is modeled and then solved analytically within the long wavelength approximation. The pressure gradient, pressure rise, friction force, stream function, shear stress, and velocity are derived and discussed. Numerical calculations are carried out and illustrated graphically in each case considered. The magnetic field and rotation may be utilized as transport of bio-fluid in ureters, intestines and arterioles. Comparison is made with existing results.

## 2. Basic equations

The basic vector equations governing the flow of a second-order fluid through a porous medium in a rotating frame are

$$\overline{\boldsymbol{\nabla}}\cdot\overline{\boldsymbol{V}}=0, \tag{1}$$

$$\rho\frac{\mathrm{D}\overline{\boldsymbol{V}}}{\mathrm{D}t}+\rho\left[\overline{\boldsymbol{\Omega}}\times(\overline{\boldsymbol{\Omega}}\times\overline{\boldsymbol{V}})+2\overline{\boldsymbol{\Omega}}\times\frac{\partial\overline{\boldsymbol{V}}}{\partial t}\right]=\overline{\boldsymbol{\nabla}}\cdot\overline{\boldsymbol{T}}-\frac{\mu}{\overline{K}}\overline{\boldsymbol{V}}+\rho\overline{f}-eP_0^2\overline{U}, \tag{2}$$

where $\rho$ is the density, $\overline{\boldsymbol{\Omega}}=\Omega\boldsymbol{k}$, $\boldsymbol{k}$ is the unit vector parallel to the $z$ axis, $\Omega$ is the rotation, $\overline{\boldsymbol{V}}$ is the velocity vector, $\overline{K}$ is the permeability of the porous medium, $\overline{f}$ is the body force, $e$ is the coefficient of electrical conductivity, $P_0$ is the magnetic field, $\mathrm{D}/\mathrm{D}t$ denotes the material derivative, and $\overline{\boldsymbol{T}}$ is the Cauchy stress tensor. The constitutive equation for an incompressible fluid of second order can be expressed as[31]

$$\overline{\boldsymbol{T}}=-\overline{p}\boldsymbol{I}+\sum_{i=1}^{2}\overline{\boldsymbol{S}}_i, \tag{3}$$

$$\overline{\boldsymbol{S}}_1=\mu\overline{\boldsymbol{A}}_1, \tag{4}$$

$$\overline{\boldsymbol{S}}_2=\alpha_1\overline{\boldsymbol{A}}_2+\alpha_2\overline{\boldsymbol{A}}_1^2, \tag{5}$$

where $\overline{p}$ is the pressure, $\boldsymbol{I}$ is an identity tensor, $\mu$ is the coefficient of viscosity, $\overline{\boldsymbol{S}}$ is the extra stress, $\alpha_1$ and $\alpha_2$ are the material constants, and $\overline{\boldsymbol{A}_1}$ and $\overline{\boldsymbol{A}_2}$ are the Rivlin–Ericksen tensors and given by

$$\overline{\boldsymbol{A}}_1=(\overline{\boldsymbol{\nabla}}\,\overline{\boldsymbol{V}})+(\overline{\boldsymbol{\nabla}}\,\overline{\boldsymbol{V}})^T,$$
$$\overline{\boldsymbol{A}}_2=\overline{\boldsymbol{A}}_{1t}+\overline{\boldsymbol{V}}\cdot\overline{\boldsymbol{\nabla}}\,\overline{\boldsymbol{A}}_1+\overline{\boldsymbol{A}}_1\cdot\overline{\boldsymbol{\nabla}}\,\overline{\boldsymbol{V}}+(\overline{\boldsymbol{A}}_1\cdot\overline{\boldsymbol{\nabla}}\,\overline{\boldsymbol{V}})^T. \tag{6}$$

## 3. Formulation of the problem

Let us consider the peristaltic transport of a second-order fluid through a porous medium. In the laboratory, we chose the Cartesian coordinates system $(\overline{\boldsymbol{X}},\overline{\boldsymbol{Y}})$ for the channel with $\overline{\boldsymbol{X}}$ along the center line and $\overline{\boldsymbol{Y}}$ transverse it, the motion of an incompressible viscous second-order fluid in a channel induced by sinusoidal wave trains propagating with constant speed $c$ along the channel walls. The geometry of the wall surface is represented by

$$\overline{h}(\overline{\boldsymbol{X}},\overline{t})=a+b\sin\frac{2\pi}{\lambda}(\overline{\boldsymbol{X}}-c\overline{t}), \tag{7}$$

where $a$ is the half width of the channel, $b$ is the wave amplitude, $\lambda$ is the wavelength, $c$ is the propagation velocity, and $\bar{t}$ is the time.

Introducing a wave frame $(\overline{x},\overline{y})$ moving with velocity $c$ away from the fixed frame $(\overline{X},\overline{Y})$ by the transformation

$$\begin{aligned}&\overline{x}=\overline{X}-c\bar{t},\quad \overline{y}=\overline{Y},\quad \overline{u}=\overline{U}-c,\\&\overline{v}=\overline{V},\quad \overline{p}(\overline{x})=\overline{P}(\overline{X},\bar{t}),\end{aligned}\tag{8}$$

where $\overline{u}$ and $\overline{v}$ are the dimensional velocity components in the direction of $\overline{x}$ and $\overline{y}$, respectively, $\overline{p}$ and $\overline{P}$ are pressures in wave and fixed frame, respectively. The pressure $\overline{p}$ remains a constant across any axial station of the channel under the assumption that the wavelength is large.

In a laboratory frame, the governing equations are reduced to the following form:

$$\frac{\partial\overline{u}}{\partial\overline{x}}+\frac{\partial\overline{v}}{\partial\overline{y}}=0,\tag{9}$$

$$\begin{aligned}&\rho\left[\overline{u}\frac{\partial\overline{u}}{\partial\overline{x}}+\overline{v}\frac{\partial\overline{u}}{\partial\overline{y}}\right]-\rho\Omega\left(\Omega\overline{u}+2\frac{\partial\overline{v}}{\partial\bar{t}}\right)\\&=-\frac{\partial\overline{p}}{\partial\overline{x}}+\frac{\partial\overline{S}_{11}}{\partial\overline{x}}+\frac{\partial\overline{S}_{12}}{\partial\overline{y}}\\&\quad-\frac{\mu}{\overline{K}}(\overline{u}-c)-eP_0^2\overline{u},\end{aligned}\tag{10}$$

$$\begin{aligned}&\rho\left[\overline{u}\frac{\partial\overline{v}}{\partial\overline{x}}+\overline{v}\frac{\partial\overline{v}}{\partial\overline{y}}\right]-\rho\Omega\left(\Omega\overline{v}-2\frac{\partial\overline{u}}{\partial\bar{t}}\right)\\&=-\frac{\partial\overline{p}}{\partial\overline{y}}+\frac{\partial\overline{S}_{12}}{\partial\overline{x}}+\frac{\partial\overline{S}_{22}}{\partial\overline{y}}-\frac{\mu}{\overline{K}}(\overline{v}).\end{aligned}\tag{11}$$

Let us consider the following dimensionless variables:

$$\begin{aligned}x&=\frac{\overline{x}}{\lambda},\quad y=\frac{\overline{y}}{a},\quad u=\frac{\overline{u}}{c},\quad v=\frac{\overline{v}}{c},\\p&=\frac{a^2\overline{p}}{c\lambda\mu},\quad S=\frac{a\overline{S}}{\mu c},\quad t=\frac{c\bar{t}}{\lambda},\quad h=\frac{\overline{h}}{a}.\end{aligned}\tag{12}$$

Using Eqs. (7) and (12), we obtain from Eqs. (9)–(11) that

$$y=h(x)=1+\phi\sin[2\pi x],\tag{13}$$

$$\delta\frac{\partial u}{\partial x}+\frac{\partial v}{\partial y}=0,\tag{14}$$

$$\begin{aligned}&\mathrm{Re}\delta\left[u\frac{\partial u}{\partial x}+\frac{1}{\delta}v\frac{\partial u}{\partial y}\right]-\left(\frac{\rho a^2\Omega^2}{\mu}u+2\delta\mathrm{Re}\Omega\frac{\partial v}{\partial t}\right)\\&=-\frac{\partial p}{\partial x}+\delta\frac{\partial S_{11}}{\partial x}+\frac{\partial S_{12}}{\partial y}-\sigma^2(u+1)-\frac{eP_0^2a^2}{\mu}u,\end{aligned}\tag{15}$$

$$\begin{aligned}&\mathrm{Re}\delta^2\left[u\frac{\partial v}{\partial x}+\frac{1}{\delta}v\frac{\partial v}{\partial y}\right]-\delta\left(\frac{\rho a^2\Omega^2}{\mu}v-2\delta\mathrm{Re}\Omega\frac{\partial u}{\partial t}\right)\\&=-\frac{\partial p}{\partial y}+\delta^2\frac{\partial S_{12}}{\partial x}+\delta\frac{\partial S_{22}}{\partial y}-\sigma^2\delta v,\end{aligned}\tag{16}$$

where

$$\begin{aligned}S_{11}&=\frac{\lambda}{a}p-2\delta\frac{\partial u}{\partial x}+\beta_1\left(2\delta^2\frac{\partial^2u}{\partial x\partial t}+2\delta^2u\frac{\partial^2u}{\partial x^2}\right.\\&\quad\left.+2\delta v\frac{\partial^2u}{\partial x\partial\overline{y}}+4\delta^2\left(\frac{\partial u}{\partial x}\right)^2+2\delta\frac{\partial v}{\partial x}\frac{\partial u}{\partial y}\right.\\&\quad\left.+2\delta^2\left(\frac{\partial v}{\partial x}\right)^2\right)+\beta_2\left(4\delta^2\left(\frac{\partial u}{\partial x}\right)^2+\left(\frac{\partial u}{\partial y}\right)^2\right.\\&\quad\left.+\delta^2\left(\frac{\partial v}{\partial x}\right)^2+2\delta\frac{\partial u}{\partial y}\frac{\partial v}{\partial x}\right),\end{aligned}\tag{17}$$

$$\begin{aligned}S_{12}&=\left(\frac{\partial u}{\partial y}+\delta\frac{\partial v}{\partial x}\right)+\beta_1\left(\delta\frac{\partial^2u}{\partial y\partial t}+\delta u\frac{\partial^2u}{\partial x\partial y}\right.\\&\quad\left.+v\frac{\partial^2u}{\partial y^2}+\delta^2\frac{\partial^2v}{\partial x\partial t}+\delta^2u\frac{\partial^2v}{\partial x^2}-\delta^2v\frac{\partial^2u}{\partial x^2}\right.\\&\quad\left.+2\delta\frac{\partial u}{\partial x}\frac{\partial u}{\partial y}-2\delta^2\frac{\partial v}{\partial x}\frac{\partial u}{\partial x}\right),\end{aligned}\tag{18}$$

$$\begin{aligned}S_{22}&=\frac{\lambda}{a}p+2\delta\frac{\partial u}{\partial x}+\beta_1\left(-2\delta^2\frac{\partial^2u}{\partial x\partial t}-2\delta^2u\frac{\partial^2u}{\partial x^2}\right.\\&\quad\left.-2\delta v\frac{\partial^2u}{\partial x\partial y}+4\delta^2\left(\frac{\partial u}{\partial x}\right)^2\right.\\&\quad\left.+2\delta\frac{\partial v}{\partial x}\frac{\partial u}{\partial y}+2\left(\frac{\partial u}{\partial y}\right)^2\right)+\beta_2\left(4\delta^2\left(\frac{\partial u}{\partial x}\right)^2+\left(\frac{\partial u}{\partial y}\right)^2\right.\\&\quad\left.+\delta^2\left(\frac{\partial v}{\partial x}\right)^2+2\delta\frac{\partial u}{\partial y}\frac{\partial v}{\partial x}\right),\end{aligned}\tag{19}$$

with dimensionless parameters

$$\begin{aligned}&\phi=\frac{b}{a},\quad \delta=\frac{a}{\lambda},\quad \sigma^2=\frac{a^2}{\overline{K}},\\&\mathrm{Re}=\frac{ca\rho}{\mu},\quad \beta_1=\frac{\alpha_1c}{\mu a},\quad \beta_2=\frac{\alpha_2c}{\mu a},\end{aligned}\tag{20}$$

where $\phi$ is the amplitude ratio, $\delta$ is the dimensionless wave number, $\sigma^2$ is the porosity parameter, Re is the Reynolds number, and $\beta_1$ and $\beta_2$ are Newtonian parameters.

Introducing the dimensionless stream function $\psi(x,y)$ such that

$$u=\frac{\partial\psi}{\partial y},\quad v=-\delta\frac{\partial\psi}{\partial x}.\tag{21}$$

We find that Eq. (14) is satisfied identically. The compatibility equation which governs the flow in terms of the stream function $\psi(x,y)$ after eliminating the pressure gradient from Eqs. (15) and (16) and then introducing Eqs. (17)–(19), we obtain

$$\begin{aligned}&\mathrm{Re}\delta\left[\psi_x\frac{\partial}{\partial x}-\psi_x\frac{\partial}{\partial y}\right]\nabla^2\psi-2\delta^2(\delta-1)\mathrm{Re}\Omega\psi_{xyt}\\&=\psi_{yyyy}+\delta^4\psi_{xxxx}-2\delta^2\psi_{xxyy}\\&\quad-\left(\frac{eP_0^2a^2}{\mu}-\frac{\rho a^2\Omega^2}{\mu}\right)\psi_{yy}+2\delta^2(\delta-1)\mathrm{Re}\Omega\psi_{xyt}\\&\quad-\sigma^2\nabla^2\psi+\frac{\rho a^2\Omega^2\delta^2}{\mu}\psi_{xx}+2\delta\frac{\partial^2}{\partial x\partial y}\\&\quad\times\left\{\beta_1(2\delta^2\psi_y\psi_{xxy}-2\delta^2\psi_x\psi_{xyy}+\delta^2(\psi_{xx})^2-(\psi_{yy})^2)\right\}\\&\quad-\delta\left(\delta\frac{\partial^2}{\partial x^2}-\frac{\partial^2}{\partial y^2}\right)\{\beta_1(\psi_y\psi_{xyy}-\psi_x\psi_{yyy}\\&\quad-\delta^2\psi_y\psi_{xxx}+\delta^2\psi_x\psi_{xxy}+2\psi_{xy}\psi_{yy}+2\delta^2(\psi_{xx})^2\}.\end{aligned}\tag{22}$$

Equation (15) for the axial pressure gradient changes into

$$\begin{aligned}
&\mathrm{Re}\delta\left[\psi_y\frac{\partial}{\partial x}-\psi_x\frac{\partial}{\partial y}\right]\psi_y+2\delta^2\mathrm{Re}\Omega\psi_{xt}\\
&=-\frac{\partial p}{\partial x}+\psi_{yyy}+\delta\frac{\partial}{\partial x}\{-2\delta\psi_{xy}+\beta_1(2\delta^2\psi_y\psi_{xxy}\\
&\quad-2\delta^2\psi_x\psi_{xyy}+4\delta^2(\psi_{xy})^2-2\delta^2\psi_{xx}\psi_{yy}+2\delta^4(\psi_{xx})^2)\\
&\quad+\beta_2(4\delta^2(\psi_{xy})^2+(\psi_{yy})^2+\delta^4(\psi_{xx})^2-2\delta^2\psi_{yy}\psi_{xx})\}\\
&\quad+\frac{\partial}{\partial y}\{-\delta^2\psi_{xx}+\beta_1(\delta\psi_y\psi_{xyy}-\delta\psi_x\psi_{yyy}-\delta^3\psi_y\psi_{xxx}\\
&\quad+\delta^3\psi_x\psi_{xxy}+2\delta\psi_{xy}\psi_{yy}+2\delta^3(\psi_{xx})^2)\}\\
&\quad-\left(\sigma^2+\frac{ep_0^2a^2}{\mu}-\frac{\rho a^2\Omega^2}{\mu}\right)\psi_y-\sigma^2, \qquad (23)
\end{aligned}$$

where

$$\nabla^2\psi=\delta^2\frac{\partial^2\psi}{\partial x^2}+\frac{\partial^2\psi}{\partial y^2}.$$

## 4. Rate of volume flow and boundary conditions

The instantaneous volume rate of flow in the fixed $(\overline{X},\overline{Y})$ coordinate system is given by

$$Q=\int_0^{\overline{h}(\overline{X},t)}\overline{U}(\overline{X},\overline{Y},t)\,\mathrm{d}\overline{Y}, \qquad (24)$$

and in the wave frame equation (24) is given by

$$q=\int_0^{\overline{h}}\overline{u}(\overline{x},\overline{y})\,\mathrm{d}\overline{y}, \qquad (25)$$

where $\overline{h}$ is a function of $\overline{x}$ alone.

Substituting Eq. (8) into Eq. (24) and using Eq. (25), we find that the two rates of volume flow are

$$Q=q+cah. \qquad (26)$$

The time mean flow over a period $T$ at a fixed position $\overline{X}$ is defined as

$$\overline{Q}=\frac{1}{T}\int_0^T Q\,\mathrm{d}t. \qquad (27)$$

Substituting Eq. (26) into Eq. (27) and integrating it, we obtain

$$\overline{Q}=q+ac. \qquad (28)$$

The dimensionless time-mean flows $\theta$ and $F$ in the fixed wave frame as

$$\theta=\frac{\overline{Q}}{ac},\quad F=\frac{q}{ac}, \qquad (29)$$

then Eq. (28) may be rewritten as

$$\theta=F+1, \qquad (30)$$

where

$$F=\int_0^{\bar{h}}\frac{\partial\psi}{\partial y}\,\mathrm{d}y=\psi(h)-\psi(0). \qquad (31)$$

Assuming the streamline equals zero $(\psi=0)$ along the central line $(y=0)$, then the wall $(y=h)$ is the stream line of value $(w=F)$.

The boundary conditions for the stream functions in the wave frame are

$$\begin{aligned}
\psi&=0,\quad \frac{\partial^2\psi}{\partial y^2}=0,\quad \text{at}\quad y=0,\\
\psi&=F,\quad \frac{\partial\psi}{\partial y}=-1,\quad \text{at}\quad y=h(x). \qquad (32)
\end{aligned}$$

Then, the boundary conditions are sufficient to determine the flow field of a Newtonian fluid. In general, the equations of motion for a second-order fluid, which are of higher order than the Navier–Stokes equations, require additional boundary conditions.

Using the long wavelength approximation and neglecting the wave number $\delta$ along with low Reynolds number in our analysis, the field equations (22) and (23) now become

$$\psi_{yyyy}-g\psi_{yy}=0, \qquad (33)$$

$$\frac{\partial p}{\partial x}=\psi_{yyy}-g\psi_y-\sigma^2, \qquad (34)$$

where

$$g=\left(\sigma^2+\frac{eP_0^2a^2}{\mu}-\frac{\rho a^2\Omega^2}{\mu}\right).$$

The solutions of Eqs. (33) and (34) subject to the boundary conditions (32) are given by

$$\psi=ny+s\sinh(\sqrt{g}y), \qquad (35)$$

$$\frac{\mathrm{d}p}{\mathrm{d}x}=-ng-\sigma^2, \qquad (36)$$

where

$$\begin{aligned}
n&=-\left(1+\frac{\sqrt{g}\cosh\left[\sqrt{g}h(x)\right]\left[F+h(x)\right]}{\sinh\left[\sqrt{g}h(x)\right]-\sqrt{g}h(x)\cosh\left[\sqrt{g}h(x)\right]}\right),\\
s&=\frac{F+h(x)}{\sinh\left[\sqrt{g}h(x)\right]-\sqrt{g}h(x)\cosh\left[\sqrt{g}h(x)\right]}.
\end{aligned}$$

The pressure rise $\Delta P_\lambda$ and the friction force $F_\lambda$ for a channel of length $L$, in their dimensionless forms, are given by

$$\Delta P=\int_0^1\frac{\mathrm{d}p}{\mathrm{d}x}\mathrm{d}x, \qquad (37)$$

$$F_\lambda=\int_0^1-h^2\frac{\mathrm{d}p}{\mathrm{d}x}\mathrm{d}x. \qquad (38)$$

Using Eq. (21), we can obtain

$$u=y+s\sqrt{g}\cosh\sqrt{g}y. \qquad (39)$$

The shear stress at $y=h(x)=1+\phi\sin(2\pi x)$ is given by

$$\overline{\tau}_{xy}=\frac{S_{12}(1-(\mathrm{d}y/\mathrm{d}x)^2)+(S_{22}-S_{11})\mathrm{d}y/\mathrm{d}x}{(1+(\mathrm{d}y/\mathrm{d}x)^2)}. \qquad (40)$$

The shear stress in the dimensionless form can be obtained from Eq. (40) in the following form:

$$\overline{\tau}_{xy}=\frac{\mu c}{a}\tau_{xy}=\frac{\mathrm{Re}\mu^2}{\rho a^2}\tau_{xy}, \qquad (41)$$

$$\tau_{xy} = \frac{\mathrm{Re}\mu^2 sg \sinh\sqrt{\bar{g}}h(x)[(1-h_x{}^2(x))+2\beta_1 sgh_x \sinh\sqrt{\bar{g}}h(x)]}{\rho a^2(1+h_x{}^2(x))}, \tag{42}$$

$$\tau_{xy} = \frac{\mathrm{Re}\mu^2 sg \sinh\sqrt{\bar{g}}h(x)[(1-4\pi^2\phi^2\cos(2\pi x)^2)+4\pi\phi\beta_1 sg \sinh\sqrt{\bar{g}}h(x)\cos(2\pi x))]}{\rho a^2(1+4\pi^2\phi^2\cos(2\pi x)^2)}. \tag{43}$$

## 5. Special case

If the porosity parameter is neglected (i.e., $\sigma^2 = 0$), we obtain the following results:

$$\psi = n_0 y + s_0 \sinh\sqrt{g_0}y, \tag{44}$$

$$\frac{\mathrm{d}p}{\mathrm{d}x} = -n_0 g_0, \tag{45}$$

$$u = y + s_0\sqrt{g_0}\cosh\sqrt{g_0}y, \tag{46}$$

$$\tau_{xy} = \frac{\mathrm{Re}\mu^2 s_0 g_0 \sinh\sqrt{g_0}h(x)[(1-4\pi^2\phi^2\cos(2\pi x)^2)+4\pi\phi\beta_1 s_0 g_0 \sinh\sqrt{g_0}h(x)\cos(2\pi x))]}{\rho a^2(1+4\pi^2\phi^2\cos(2\pi x)^2)}, \tag{47}$$

where

$$s_0 = \frac{F+h(x)}{\sinh\left[\sqrt{g_0}h(x)\right]-\sqrt{g_0}h(x)\cosh\left[\sqrt{g_0}h(x)\right]},$$

$$n_0 = -\left(1+\frac{\sqrt{g_0}\cosh\left[\sqrt{g_0}h(x)\right][F+h(x)]}{\sinh\left[\sqrt{g_0}h(x)\right]-\sqrt{g_0}h(x)\cosh\left[\sqrt{g_0}h(x)\right]}\right),$$

$$g_0 = \left(\frac{eP_0^2a^2}{\mu}-\frac{\rho a^2\Omega^2}{\mu}\right).$$

## 6. Numerical results and discussion

In order to gain physical insight into the pressure gradient $|\mathrm{d}p/\mathrm{d}x|$, pressure rise $|\Delta P_\lambda|$, friction force $|F_\lambda|$, stream function $|\psi|$, shear stress $|\tau_{xy}|$, and velocity $|u|$ have been discussed by assigning numerical values to the parameter encountered in the problem in which the numerical results are displayed with the graphic illustrations. The variations are shown in Figs. 1–12, respectively, with the constant values $a = 0.2$, $e = 2$, $F = -10$, $p_0 = 5$, $\mathrm{Re} = 1.71$, $x = 0.7$, $\phi = 0.5$, $\beta_1 = -0.8$, $\mu = 0.4$, $\rho = 1.057$ and $\Omega = 0.5$.

Figure 1 shows the variations of the absolute value of pressure gradient $|\mathrm{d}p/\mathrm{d}x|$ with respect to $x$, which exhibits oscillatory behavior in the whole range of $x$ for different values of the non-dimensional wave amplitude $\phi$, porosity $\sigma$, magnetic field $P_0$, rotation $\Omega$, and the dimensionless time-mean flow in the wave frame $F$. It is clear that the pressure gradient $|\mathrm{d}p/\mathrm{d}x|$ has a nonzero value only in a bounded region of space. The effects of the non-dimensional wave amplitude, porosity, magnetic field, rotation, and the dimensionless time-mean flow in the wave frame on the pressure gradient first decrease and then increase gradually. It is observed that the pressure gradient increases with increasing non-dimensional wave amplitude, porosity, and magnetic field, while it decreases with increasing rotation and dimensionless time-mean flow in the wave frame. It is also found that $|\mathrm{d}p/\mathrm{d}x|$ intersects when the effect of the non-dimensional wave amplitude at $x = 0.5$ decreases at $0 \le x \le 0.5$, while increases at $0.5 \le x \le 1$.

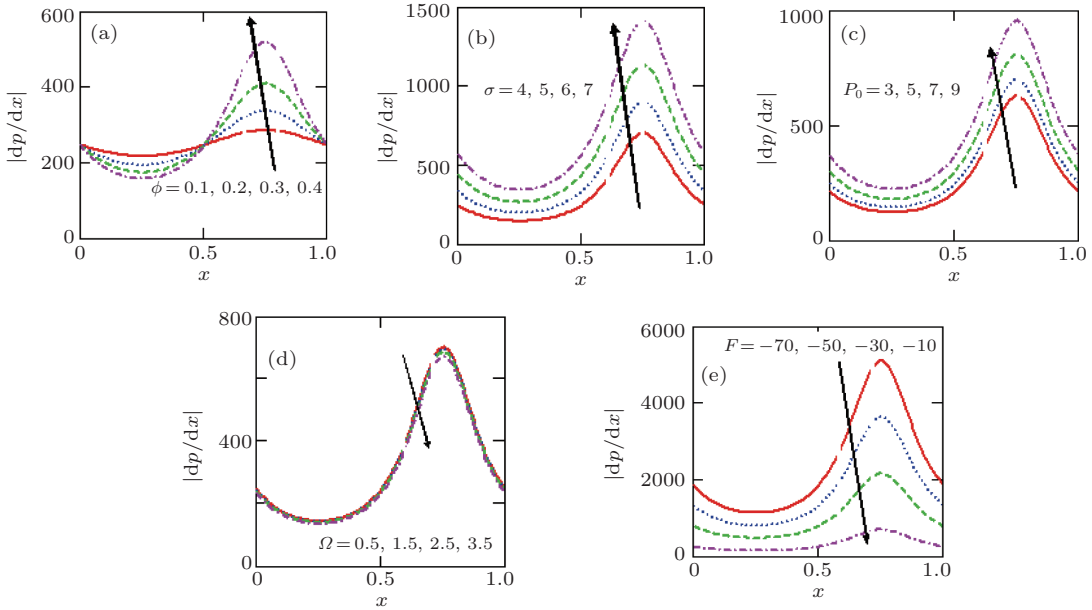



**Fig. 1.** (color online) Variations of pressure gradient ratio $|\mathrm{d}p/\mathrm{d}x|$ with respect to $x$ for different values of (a) $\phi$, (b) $\sigma$, (c) $P_0$, (d) $\Omega$, and (e) $F$.

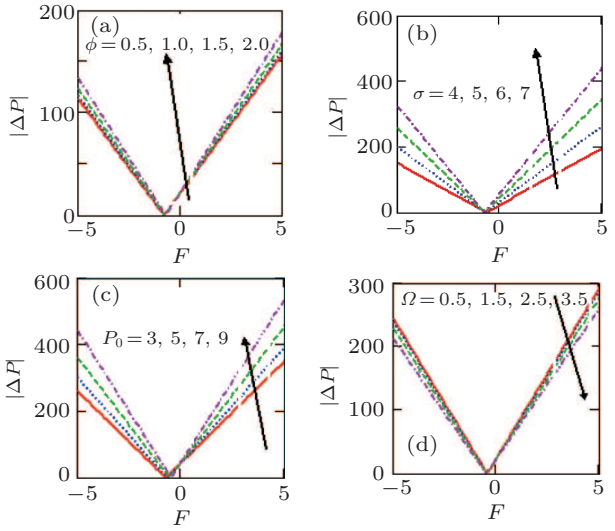



**Fig. 2.** (color online) Variations of pressure rise $|\Delta P|$ with respect to $F$ for different values of (a) $\phi$, (b) $\sigma$, (c) $P_0$, and (d) $\Omega$.

Figures 2 and 3 show the variations of the absolute value of pressure rise $|\Delta P_\lambda|$ and the absolute value of friction force $|F_\lambda|$, respectively, with respect to the dimensionless time-mean flow in wave frame $F$. Reflection and refraction occur at $F = 0$ for different values of the porosity $\sigma$ and magnetic field $P_0$ except the effects of the non-dimensional wave amplitude $\phi$ and the rotation $\Omega$ at $F = -1$. In both figures, it is clear that the absolute value of pressure rise and the absolute value of friction force have a nonzero value only in a bounded region of space. The effects of non-dimensional wave amplitude, porosity, magnetic field, and rotation on the absolute value of pressure rise and the absolute value of friction force first decrease and then increase gradually. It is observed that the absolute value of pressure rise and the absolute value of friction force increase with increasing non-dimensional wave amplitude, porosity, and magnetic field, while they decrease with increasing rotation. It is found that the absolute value of pressure rise $|\Delta P_\lambda|$ and the absolute value of friction force $|F_\lambda|$, respectively, are reflected within $-5 \le F \le 0$ and are refracted within $0 \le F \le 5$ for all four values of $\phi, \sigma, P_0$, and $\Omega$.

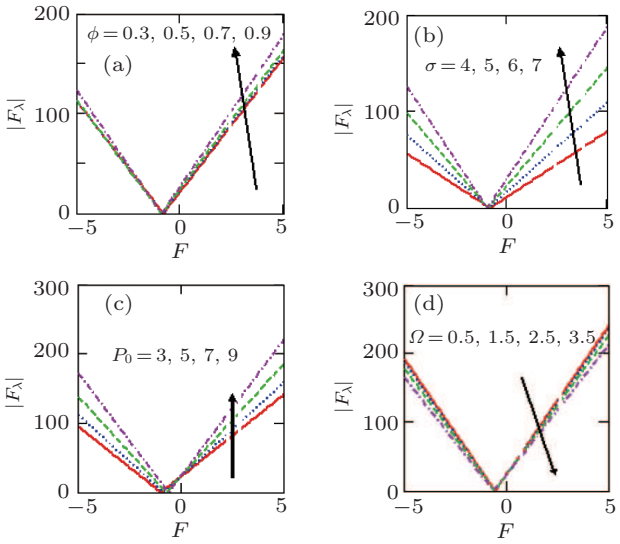



**Fig. 3.** (color online) Variations of frictional forces $|F_\lambda|$ with respect to $F$ for different values of (a) $\phi$, (b) $\sigma$, (c) $P_0$, and (d) $\Omega$.

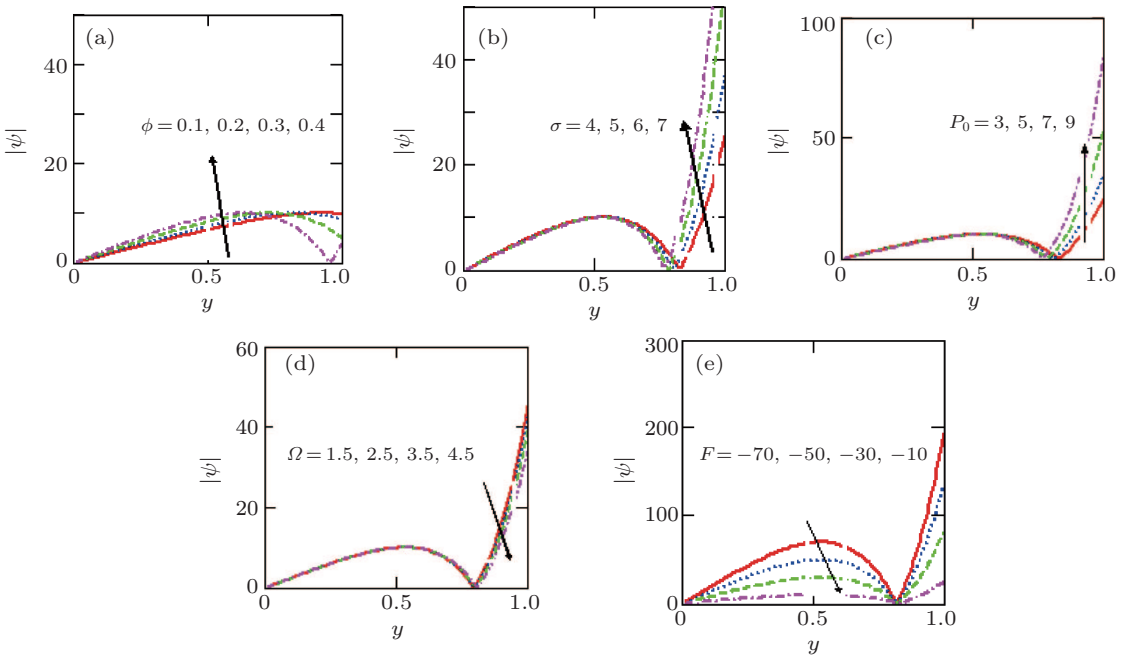



**Fig. 4.** (color online) Variations of stream function $|\psi|$ with respect to $y$ for different values of (a) $\phi$, (b) $\sigma$, (c) $P_0$, (d) $\Omega$, and (e) $F$.

Figure 4 shows the variations of the absolute value of stream function $|\psi|$ with respect to $y$, which has oscillatory behavior in the whole range of the $y$ axis, and is reflected and refracted at $y = 0$, 0.8 for different values of the porosity $\sigma$, magnetic field $P_0$, rotation $\Omega$, and the dimensionless time-mean flow in wave frame $F$ except when the effects of non-dimensional wave amplitude $\phi$ at $y = 0.95$. It is clear from Fig. 4 that the absolute value of stream function has a nonzero value only in a bounded region of space. The effects of non-dimensional wave amplitude, porosity, magnetic field, rotation, and dimensionless time-mean flow first decrease and then increase gradually. It is observed that the absolute value of stream function decreases with increasing rotation and dimensionless time-mean flow, while it increases with increasing non-dimensional wave amplitude, the porosity, and magnetic field.

Figure 5 shows the variations of the absolute value of shear stress $|\tau_{xy}|$ with respect to $x$, which exhibits oscillatory behavior in the whole range of the $x$ axis for different values of the non-dimensional wave amplitude $\phi$, porosity $\sigma$, magnetic field $P_0$, rotation $\Omega$, dimensionless time-mean flow in wave frame $F$, and the Newtonian parameter $\beta_1$. It is clear from Fig. 5 that the absolute value of shear stress has a nonzero value only in a bounded region of space. The effects of non-dimensional wave amplitude, porosity, magnetic field, rotation, dimensionless time-mean flow, and Newtonian parameter in wave frame first decrease and then increase gradually. It is observed that the absolute value of shear stress decreases with increasing rotation, dimensionless time-mean flow, and the Newtonian parameter, while it increases with increasing values of non-dimensional wave amplitude, porosity, and magnetic field. It is noted that the values of shear stress are very small at $x = 0.25$ and 0.75 for the effects of non-dimensional wave amplitude, magnetic field, porosity, rotation, dimensionless time-mean flow in wave frame, and Newtonian parameter.

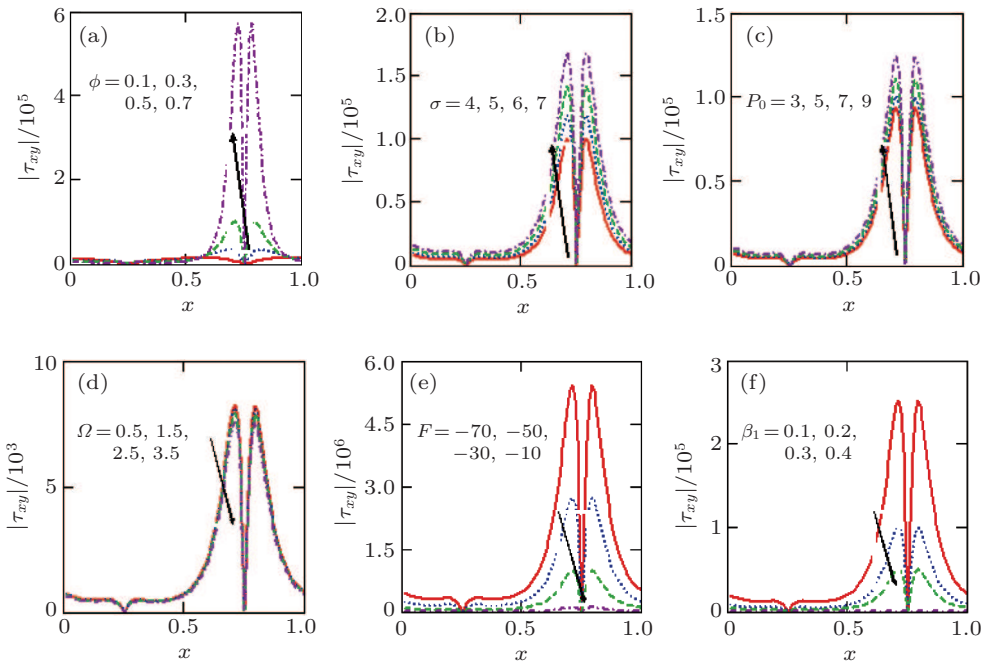



**Fig. 5.** (color online) Variations of shear stress $|\tau_{xy}|$ with respect to $x$ for different values of (a) $\phi$, (b) $\sigma$, (c) $P_0$, (d) $\Omega$, (e) $F$, and (f) $\beta_1$.

Figure 6 shows the variations of the absolute value of velocity $|u|$ with respect to $y$, which reveal oscillatory behavior in the whole range of the $y$ axis, and vanish at $y \approx 0.55$ for different values of non-dimensional wave amplitude $\phi$, porosity $\sigma$, magnetic field $P_0$, rotation $\Omega$, and dimensionless time-mean flow in wave frame $F$. It is clear that the velocity has a nonzero value only in a bounded region of space. The effects of the non-dimensional wave amplitude, porosity, magnetic field, rotation and dimensionless time-mean flow on velocity decreases and increases gradually with increasing of $y$. It is obvious that the velocity increases with increasing the non-dimensional wave amplitude, the porosity and magnetic field, while it decreases with increasing the rotation and the dimensionless time-mean flow.

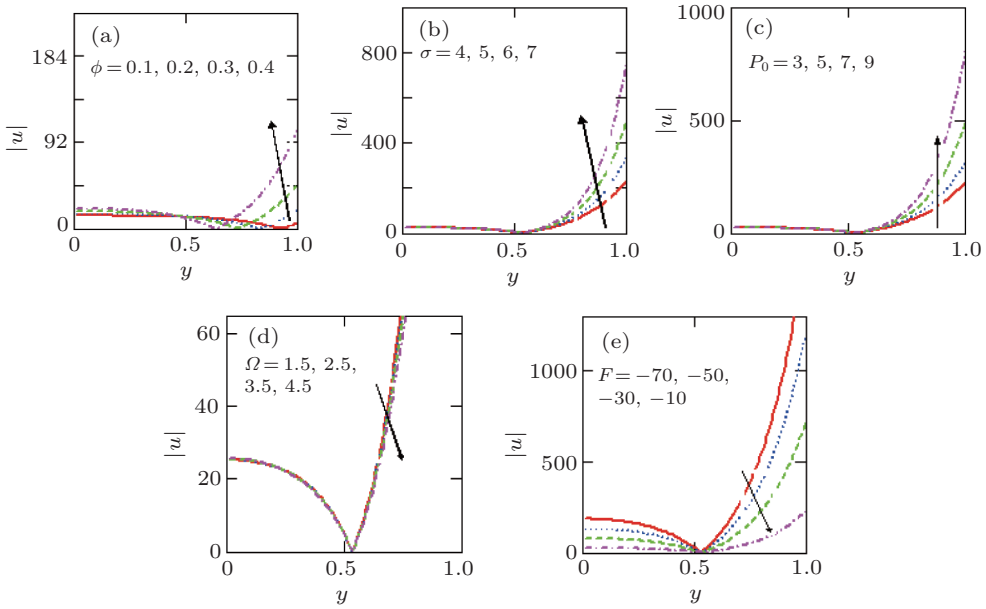



**Fig. 6.** (color online) Variations of velocity $|u|$ with respect to $y$ for different values of (a) $\phi$, (b) $\sigma$, (c) $P_0$, (d) $\Omega$, and (e) $F$.

Figure 7 displays the variations of the absolute values of the pressure gradient $|\mathrm{d}p/\mathrm{d}x|$ with respect to $x$, which has oscillatory behavior in the whole range of the $x$ axis for different values of the non-dimensional wave amplitude $\phi$ ($e = 0.3$), magnetic field $P_0$, rotation $\Omega$ and the dimensionless time-mean flow $F$ in the wave frame when the porosity $\sigma$ is neglected. It appears that the pressure gradient has a nonzero value only in a bounded region of space. The effects of the non-dimensional wave amplitude, magnetic field, rotation and the dimensionless time-mean flow in the wave frame on pressure gradient which it decreases and increases gradually while it is then up to a maximum at $x = 0.8$. It is observed that the pressure gradient decreases with increasing of non-dimensional wave amplitude, rotation and the dimensionless time-mean flow,[19] while it increases with an increasing of magnetic field.

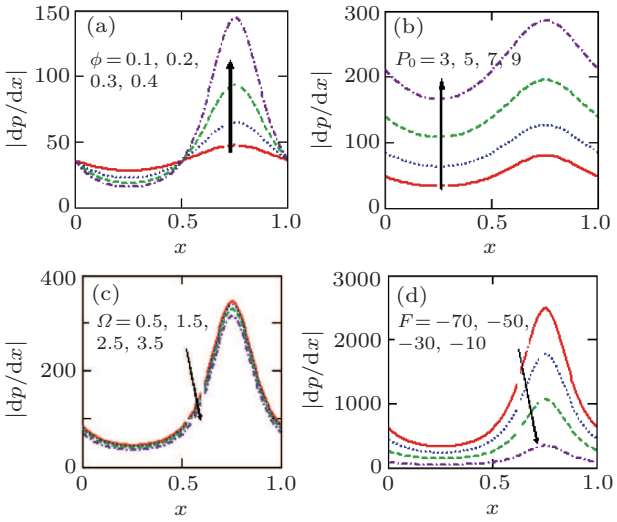



**Fig. 7.** (color online) Variations of pressure gradient ratio $|\mathrm{d}p/\mathrm{d}x|$ with respect to $x$ if $\sigma^2 = 0$ for different values of (a) $\phi$, (b) $P_0$, (c) $\Omega$, and (d) $F$.

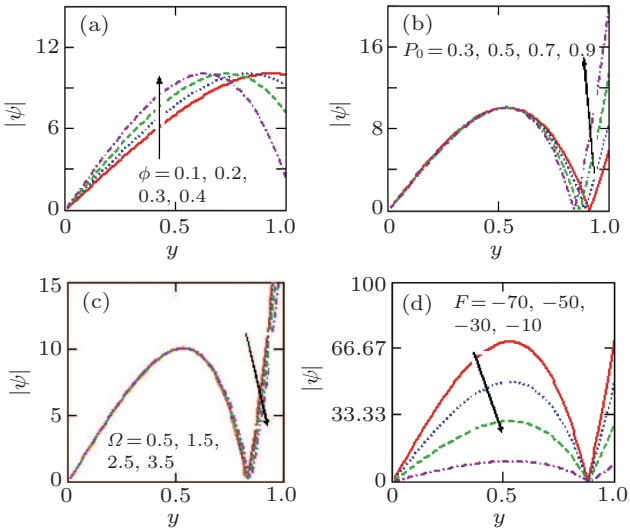



**Fig. 8.** (color online) Variations of stream function $|\psi|$ with respect to $y$ if $\sigma^2 = 0$ for different values of (a) $\phi$, (b) $P_0$, (c) $\Omega$, and (d) $F$.

Figure 8 shows the variations of the absolute value of stream function $|\psi|$ with respect to $y$ and its reflection and refraction for different values of the magnetic field $P_0$, the rotation $\Omega$ and the dimensionless time-mean flow in wave frame $F$ except when the effect of the non-dimensional wave amplitude $\phi$ there is no reflection and refraction when the porosity $\sigma$ is neglected. It is clear that the absolute value of stream function has a nonzero value only in a bounded region of space. The effects of non-dimensional wave amplitude, magnetic field, rotation, and dimensionless time-mean flow in the wave frame first increase and then decrease gradually with increasing $y$. It is shown that the absolute value of stream function decreases with increasing rotation and dimensionless time-mean flow, while it increases with increasing non-dimensional wave amplitude and magnetic field.[22]

Figure 9 shows the variations of the absolute value of shear stress $|\tau_{xy}|$ with respect to $x$ which has oscillatory behavior in the whole range of the $x$ axis for different values of the non-dimensional wave amplitude $\phi$, magnetic field $P_0$, rotation $\Omega$, dimensionless time-mean flow $F$, and the Newtonian parameter $\beta_1$ in the wave frame when the porosity $\sigma$ is neglected. It is clear that the absolute value of shear stress has a non zero value only in a bounded region of space. The effects of non-dimensional wave amplitude, magnetic field, rotation, dimensionless time-mean flow, and Newtonian parameter first decrease and then increase gradually. It is seen that the absolute value of shear stress increases with increasing values of non-dimensional wave amplitude and magnetic field, while it decreases with increasing rotation, dimensionless time-mean flow, and Newtonian parameters in the wave frame. It is noted that the shear stress is very small at $x = 0.25$ and 0.75 for the non-dimensional wave amplitude, magnetic field, rotation, dimensionless time-mean flow, and Newtonian parameter,[16] while it approaches the maximum value at $x = 0.6$ and 0.9.

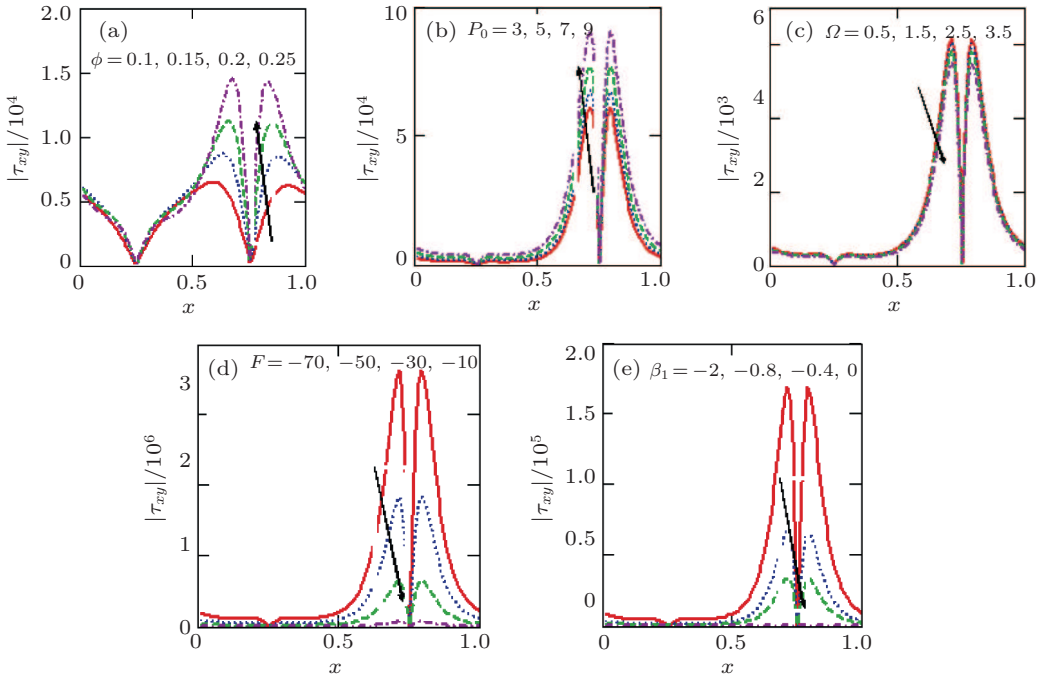



**Fig. 9.** (color online) Variations of shear stress $|\tau_{xy}|$ with respect to $x$ if $\sigma^2 = 0$ for different values of (a) $\phi$, (b) $P_0$, (c) $\Omega$, (d) $F$ and (e) $\beta_1$.

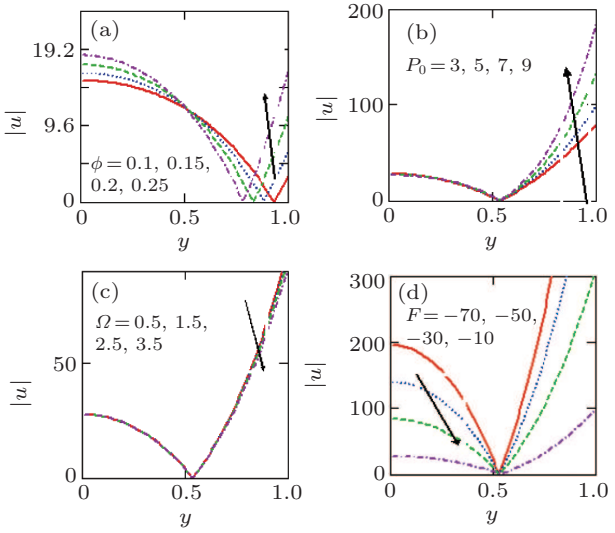



**Fig. 10.** (color online) Variations of velocity $|u|$ with respect to $y$ if $\sigma^2 = 0$ for different values of (a) $\phi$, (b) $P_0$, (c) $\Omega$, and (d) $F$.

Figure 10 shows the variations of the absolute value of velocity $|u|$ with respect to $y$ and it vanish at $y = 0.52$ except when the effect of the non-dimensional wave amplitude vanishes at $y = 0.8, 0.85, 0.9$, and 0.95 for different values of the magnetic field $P_0$, rotation $\Omega$ and the dimensionless time-mean flow in wave frame $F$ when the porosity $\sigma$ is neglected. It is clear that the velocity has a nonzero value only in a bounded region of space. The effects of non-dimensional wave amplitude, magnetic field, rotation, and dimensionless time-mean flow on the velocity first decrease and then increase gradually. It is observed that the velocity increases with increasing non-dimensional wave amplitude and magnetic field,[28] while it decreases with increasing rotation and dimensionless time-mean flow.

Figures 11 and 12 show the variations of the absolute value of pressure rise $|\Delta P_\lambda|$ and the absolute value of friction force $|F_\lambda|$, respectively, with respect to the dimensionless time-mean flow in wave frame $F$ which it reflects and refracts at $F = -0.5$ for different values of the non-dimensional wave amplitude $\phi$, magnetic field $P_0$, and the rotation $\Omega$ when the

porosity $\sigma$ is neglected. In both figures, it is clear that the absolute value of pressure rise and the absolute value of friction force have a nonzero value only in a bounded region of space. The effects of non-dimensional wave amplitude, magnetic field, and rotation on the absolute value of pressure rise and the absolute value of friction force first decrease and then increase gradually. It is observed that the absolute value of pressure rise and the absolute value of friction force increase with increasing non-dimensional wave amplitude and magnetic field,[29,30] while they decrease with increasing rotation. It is found that the absolute value of pressure rise $|\Delta P_\lambda|$ and the absolute value of friction force $|F_\lambda|$, respectively, are reflected within $-5 \le F \le 0$ and refracted within $0 \le F \le 5$ for all three values of $\phi$, $P_0$, and $\Omega$.

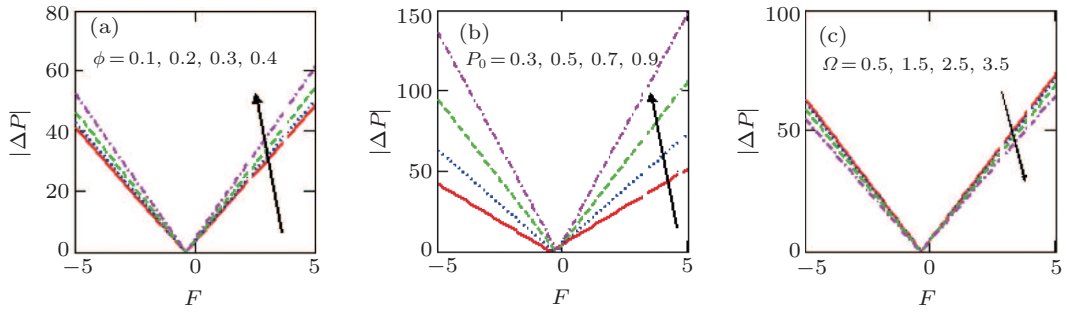



**Fig. 11.** (color online) Variations of pressure rise $|\Delta P_\lambda|$ with respect to $F$ if $\sigma^2 = 0$ for different values of (a) $\phi$, (b) $P_0$, and (c) $\Omega$.

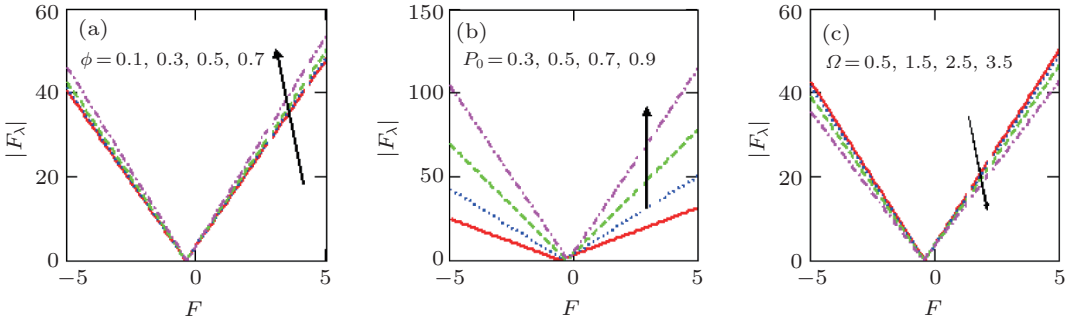



**Fig. 12.** (color online) Variations of frictional forces $|F_\lambda|$ with respect to $F$ if $\sigma^2 = 0$ for different values of (a) $\phi$, (b) $P_0$, and (c) $\Omega$.

The results indicate that the effects of non-dimensional wave amplitude, porosity, magnetic field, rotation, dimensionless time-mean flow, and Newtonian parameter are very pronounced and effective in the peristaltic phenomena.

## 7. Conclusion

Due to the complicated nature of the pertinent field equations governing peristaltic flow, a small number of works have been done in this field. The method used in this study provides a quite successful choice for dealing with such problems. This method provides exact solutions in the peristaltic flow without any assumed restrictions on the actual physical quantities that appear in the governing equations of the problem considered. Important phenomena are observed from our calculation results.

i) It is found that for large values of non-dimensional wave amplitude, porosity, magnetic field, and dimensionless time-mean flow in the wave frame. The case is quite different when we consider small values of the rotation. The solutions are obtained in the context of the peristaltic flow of second-order fluid through a porous medium.

ii) Comparing with previous studies, we find that our results (shown in Figs. 1–12) without porosity, magnetic field, and rotation coincide with the results obtained by Siddique and Schwarz[25] for non-Newtonian fluid. Also, these results agree with those of Shapiro *et al.*[26] and Shukla *et al.*[27] when the non-dimensional wave amplitude $\phi$, porosity $\sigma$, rotation $\Omega$, magnetic field $p_0$, and dimensionless time-mean flow in wave frame $F$ almost equal zero. In case of a porosity $\sigma = 0$, our results are in agreement with that of Hayat and Ali.[18] The analytical results obtained by Mishra and Ramachandra[28] can be considered as a limiting case (by taking $\sigma = 0$ and $\Omega = 0$), which are in agreement with earlier results obtained by Eytan and Elad.[29] The velocity distribution $u$ (Fig. 6) confirms the idea that peristaltic flow through a porous medium brings rigidity to the fluid.[30]

iii) The results presented in this paper should prove useful for researchers in science and engineering, as well as for

those working on the development of fluid mechanics, the non-dimensional wave amplitude, porosity, rotation, ratio of relaxation to retardation time, and dimensionless time-mean flow in wave frame exchange with the rotation influence and operations. Study of the phenomenon of the non-dimensional wave amplitude, the porosity, rotation, the ratio of relaxation to retardation time and the dimensionless time-mean flow in the wave frame are also used to improve the conditions of peristaltic motion.

## References


[1] Hayat T, Ali N and Abbas Z 2007 *Phys. Lett. A* **37** 331
[2] Siddiqui A M and Schehawey W H 1994 *J. Fluid Mech.* **53** 257
[3] Abd-Alla A M, Yahya G A, Mahmoud S R and Alosaimi H S 2012 *Meccanica* **47** 1455
[4] Mahmoud S R, Abd-Alla A M and El-Sheikh M A 2011 *Int. J. Mod. Phys. B* **25** 2713
[5] Tripathi D, Pandey S K and Das S 2011 *Acta Astronaut* **69** 30
[6] Wang Y, Ali N, Hayat T and Oberlack M 2011 *Appl. Math. Model* **35** 3737
[7] Akbar N S, Nadeem S, Hayat T and Hendi A A 2011 *Int. J. Heat Mass Tran.* **54** 4360
[8] Akbar N S, Hayat T, Nadeem S and Hendi A A 2011 *Int. J. Heat Mass Tran.* **54** 1654
[9] Gad N S 2011 *Appl. Math. Comput.* **217** 4313
[10] Nadeem S and Akbar N S 2011 *J. Taiwan Inst. Chem. Eng.* **42** 58
[11] Hayat T, Saleem N, Asghar S, Alhothuali M S and Alhomaidan A 2011 *Commun. Nonlinear Sci. Numer. Simulat.* **16** 3559
[12] Pandey S K, Chaube M K and Tripathi D 2011 *J. Theor. Biol.* **278** 11
[13] Pandey S K, Chaube M K, Nadeem S and Akram S 2010 *Commun. Nonlinear Sci. Numer. Simulat.* **15** 1705
[14] Pandey S K and Chaube M K 2010 *Math. Comput. Model.* **52** 501
[15] Haroun M H 2007 *Commun. Nonlinear Sci. Numer. Simulat.* **12** 1464
[16] Kothandapani M and Srinivas S 2008 *Phys. Lett. A* **372** 1265
[17] Hayat T, Afsar A, Khan M and Asghar S 2007 *Comput. Math. Appl.* **53** 1074
[18] Ali N, Sajid M, Abbas Z and Javed T 2010 *Eur. J. Mech. B: Fluids* **29** 387
[19] Hayat T and Ali N 2008 *Commun. Nonlinear Sci. Numer. Simulat.* **13** 1343
[20] Kothandapani M and Srinivas S 2008 *Int. J. Nonlinear Mech.* **43** 915
[21] Haroun M H 2007 *Comput. Mater. Sci.* **39** 324
[22] Hayat T, Asghar Z, Asghar S and Mesloub S 2010 *J. Taiwan Inst. Chem. Eng.* **41** 553
[23] Nadeem S and Akram S 2010 *Math. Comput. Model* **52** 107
[24] Srinivas S and Gayathri R 2009 *Appl. Math. Comput.* **215** 185
[25] Srinivas S and Pushparaj V 2008 *Commun. Nonlinear Sci. Numer. Simulat.* **13** 1782
[26] Shapiro A H, Jaffrin M Y and Weinberg S L 1969 *J. Fluid Mech.* **37** 799
[27] Shukla J B, Parihar R S, Rao B R P and Gupta S P 1980 *J. Fluid Mech.* **97** 225
[28] Mishra M, Ramachandra R and Angew Z 2003 *Z. Angew. Math. Phys.* **54** 532
[29] Eytan O and Elad D 1999 *Bull. Math. Biol.* **61** 221
[30] Mekheimer Kh S 2003 *J. Porous Media* **6** 189
[31] Coleman B D and Noll W 1960 *Arch. Rational Mech. Anal.* **6** 355